

# A Stochastic Market-based Clearing Approach in Active Distribution Networks by Using Interval Optimization

Augusto C. Rueda-Medina

Rafael S. F. Ferraz

Renato S. F. Ferraz

Oureste Elias Batista

Department of Electrical Engineering

Federal University of Espírito Santo

Vitória, Brazil

{augusto.rueda, oureste.batista}@ufes.br, {rafael.ferraz, renato.s.ferraz}@edu.ufes.br

**Abstract**—The uncertainties inherent to variations in load demand and generation from distributed energy resources, such as distributed generators (DGs) based on wind and solar radiation, introduce challenges that must be addressed in order to develop efficient electricity markets. In this work, the DGs active power generation and reserve scheduling problem in active distribution networks is solved through a proposed co-optimization market-based clearing approach, in which the volatility of the load demand and DGs with uncertainties (DG<sub>SU</sub>) are considered. Through Benders decomposition, the formulated problem is decomposed into a master problem and an interval feasibility check sub-problem, in which the interval linear programming theory is used to account for the large amount of probabilistic scenarios generated due to the stochastic characteristics of this problem. In a stage previous to the market clearing algorithm, the lower and upper bounds of the interval parameters associated to the load demand and DG<sub>SU</sub> generation are defined through an enhanced forecasting system, which uses the Markov models theory and the Monte Carlo method. Tests and comparisons with a method using probability distributions were performed using the IEEE 37-bus distribution test system to show the effectiveness of the proposed approach.

**Index Terms**—Distributed generators, distribution systems, reserves market, uncertainty.

## NOTATION

The notation used throughout this paper is reproduced below for quick reference.

Sets with corresponding subscripts (abbreviated as subs):

$\Omega_T$  hours (sub  $t$ )  
 $\Omega_{Bus}$  buses of the system (subs  $i$  or  $j$ )  
 $\Omega_{UBr}^i$  upstream branches attached to bus  $i$  (sub  $j$ )  
 $\Omega_{DBr}^i$  downstream branches attached to bus  $i$  (sub  $j$ )  
 $\Omega_{DG_U}$  distributed generators (DGs) with uncertainties (sub  $g$ )  
 $\Omega_{DG_{NU}}$  DGs with non-uncertainties (sub  $g$ )  
 $\Omega_{DG}$  all DGs (sub  $g$ ). Note that  $\Omega_{DG} = \Omega_{DG_U} \cup \Omega_{DG_{NU}}$   
 $\Omega_{Disc}$  discretizations for linearization of  $V_j^{Sq\pm}$  (sub  $u$ )

$\Omega_{Disc}^*$  set  $\Omega_{Disc}$  without the first element (sub  $u^*$ )  
 $\Omega_L$  blocks of the linearization of  $P_{ij}^{\pm 2}$  and  $Q_{ij}^{\pm 2}$  (sub  $l$ )  
 $\Omega_{St}$  load demand states (sub  $st$ )  
 $\Omega_{In}^P$  inequality active power demand constraints (sub  $q$ )  
 $\Omega_{In}^Q$  inequality reactive power demand constraints (sub  $q$ )

Constants:

$\alpha_t$  cost of active power *-dispatch-* bought by the distribution system operator (DSO) from the main grid  
 $\beta_t$  price of *reserve* sold to the main grid  
 $of_{E,g,t}, of_{R,g,t}$  DG's offers of *dispatch* and *reserve*  
 $fr_{g,t}$  *reserve* factor  
 $R_{Br,ij}, X_{Br,ij}$  branch resistance and reactance  
 $\bar{Z}_{Br,ij}$  branch impedance  
 $\bar{\Delta}_V$  discretization step of  $V_{j,t}^{Sq\pm}$   
 $\bar{\Delta}_{S,ij}$  upper bound of each power flow block  
 $m_{S,l,ij}$  slope of the  $l$ -th power flow block  
 $P_{D,i,t}^\pm, Q_{D,i,t}^\pm$  active and reactive power demand  
 $R_{Req,t}^\pm$  *reserve* requirement  
 $\overline{P_{DG,g,t}^\pm}, \overline{Q_{DG,g,t}^\pm}$  DG's maximum active and reactive power generation limits  
 $P_{h,g}, Q_{h,g}$   $h$ -th point of the linearization of the DG's capability curve  
 $\underline{V}, \bar{V}$  minimum and maximum node voltage limits  
 $\bar{I}_{ij}$  maximum branch current limit  
 $\underline{\Psi}_{In,q,t}^{P,(st)}, \bar{\Psi}_{In,q,t}^{P,(st)}$  minimum and maximum limits of an active power demand inequality constraint  
 $\underline{\Psi}_{In,q,t}^{Q,(st)}, \bar{\Psi}_{In,q,t}^{Q,(st)}$  minimum and maximum limits of a reactive power demand inequality constraint  
 $LF_t^\pm$  load factor

Variables:

$PB^\pm$  payment burden of the DSO  
 $FC^\pm$  financial compensation to the DGs  
 $FR^\pm$  financial reward of the DSO  
 $P_{SS,i,t}^\pm, Q_{SS,i,t}^\pm$  substation active and reactive power

Submitted to the 23rd Power Systems Computation Conference (PSCC 2024).

$E_{g,i,t}^{\pm}, R_{g,i,t}^{\pm}$	<i>dispatch</i> and <i>reserve</i> provided by a DG
$I_{ij,t}^{Sq\pm}$	square of the branch current
$P_{ij,t}^{\pm}, Q_{ij,t}^{\pm}$	active and reactive power flows
$V_{i,t}^{Sq\pm}$	square of the node voltage
$\pi_{V,u,j,t}^{\pm}$	binary variable for linearization of $V_j^{Sq\pm}$
$P_{C,u,j,t}^{\pm}$	power corrections
$P_{ij,t}^{\uparrow\pm}, P_{ij,t}^{\downarrow\pm}$	non-negative auxiliaries of $ P_{ij,t}^{\pm} $
$Q_{ij,t}^{\uparrow\pm}, Q_{ij,t}^{\downarrow\pm}$	non-negative auxiliaries of $ Q_{ij,t}^{\pm} $
$\Delta_{P,l,ij,t}^{\pm}, \Delta_{Q,l,ij,t}^{\pm}$	values of the $l$ -th block of $ P_{ij,t}^{\pm} $ and $ Q_{ij,t}^{\pm} $
$\xi_{E,g,i,t}^{\pm}, \xi_{R,g,i,t}^{\pm}$	<i>dispatch</i> and <i>reserve</i> market prices
$\lambda_{E,g,i,t}^{\pm}, \lambda_{R,g,i,t}^{\pm}$	<i>dispatch</i> and <i>reserve</i> marginal prices
$v$	objective function value of the interval feasibility check sub-problem
$\lambda_{B,1,i,t}^{P(st)}, \lambda_{B,2,i,t}^{P(st)}$	non-negative slack variables of an active power demand balance constraint
$\lambda_{B,1,i,t}^{Q(st)}, \lambda_{B,2,i,t}^{Q(st)}$	non-negative slack variables of a reactive power demand balance constraint
$\lambda_{In,1,q,t}^{P(st)}, \lambda_{In,2,q,t}^{P(st)}$	non-negative slack variables of an active power demand inequality constraint
$\lambda_{In,1,q,t}^{Q(st)}, \lambda_{In,2,q,t}^{Q(st)}$	non-negative slack variables of a reactive power demand inequality constraint
$\Psi_{B,i,t}^{P(st)}(\cdot), \Psi_{B,i,t}^{Q(st)}(\cdot)$	functions of an active and reactive power balance constraints
$\Psi_{In,q,t}^{P(st)}(\cdot), \Psi_{In,q,t}^{Q(st)}(\cdot)$	functions of an active and reactive power inequality constraints
$P_L^{\pm}$	total active power losses

## I. INTRODUCTION

### A. Background and Motivation

The increasing participation of distributed energy resources (DERs), such as distributed generators (DGs), transforms the electric power systems at the distribution-level into active networks, where the distribution system operator (DSO) has new possibilities including active power trading with DGs owners and scheduling of their own DGs, as well as being able to behave as a *price-maker* in the wholesale electricity market [1], [2]. In addition, the fast response of the DGs also enables the DSO to participate in the ancillary services market as a supplier of active power reserve for frequency control - which will be henceforth simply referred to as *reserve*.

According to the authors of [3], most studies on the subject are in agreement that the demand for *reserves* in several countries in Europe and the United States has increased in recent years by almost up to 10% of the additional RESs capacity. A typical case of such new types of products has been applied in Belgium, where the transmission system operator (TSO) Elia has introduced two additional *reserve* types, which belong to the wider category of tertiary *reserves* (R3), to be provided by RESs, namely: R3 dynamic profile and R3 aggregated power plant [4].

Variation of the primary energy source of DGs with high degree of uncertainty -which will be henceforth referred to as  $DG_{SU}$ - creates the need to developing stochastic market clearing problems to be solved through stochastic optimization

techniques. In this regard, several works have been developed on the transmission-level market, where the uncertainty of the  $DG_{SU}$  is strategically accommodated; however, the participation of DGs in distribution networks as providers of *reserves*, accurate operation models of the DGs' technologies, such as synchronous generators (SGs) and doubly-fed induction generators (DFIGs), and an efficient linearization of the original mixed-integer non-linear programming (MINLP) model of this problem, are commonly disregarded. Furthermore, most of those proposals provide solutions that are valid only for the time series pattern that is being applied, disregarding the existence of other patterns which are possible to happen, or by supposing values for limiting the volatility of the load demand and  $DG_{SU}$  generation, but without any previous forecasting study.

In this work, a co-optimization market-based clearing methodology is proposed to solve the problem of scheduling *reserve* and *dispatch* of the active power required to meet loads -which will be henceforth simply referred to as *dispatch*- in active distribution networks, in which the uncertainties of the load demand and wind-based  $DG_{SU}$  is considered. In this problem, the payment burden of the DSO for *dispatch* and *reserve* is minimized considering pessimistic and optimistic states in a proposed day-ahead market-based clearing algorithm (MCA). Due to the difficulty introduced by the original MINLP nature of the problem, where non-linearities are introduced by the representation of the nodal load balance, and additional computational burden related to its stochastic characteristics, the formulation of this problem is linearized and Benders decomposition [5] is implemented to decompose the original problem into an expected master problem (EMP) and an interval feasibility check sub-problem (IFChS), which provides the feasibility cuts. The interval linear programming (ILP) theory [6] is used to account for the large amount of scenarios generated in the IFChS in order to determine the pessimistic and optimistic states. To define the lower and upper bounds of the interval parameters associated to the load demand and wind in zones where the  $DG_{SU}$  are installed, an enhanced forecasting system with a reduction technique (EFS-RT) based on the forecasting methodology proposed in [7], which uses the Markov models (MkvM) theory and the Monte Carlo method (MCM), is used in a scenarios generation and reduction stage, previous to the application of the MCA.

Tests and comparisons with methods using probability distributions were performed in the IEEE 37-bus distribution test system [8] to show the effectiveness of the proposed methodology. The risks caused by the uncertainties inherent to the interval parameters are analyzed in order to establish critical operating scenarios. In this way, the proposed methodology allows the DSO to be aware of critical solutions of the co-optimization market-based problem and the limits of the corresponding risks.

### B. State of the Art and Contributions

The distribution-level electricity market, operated by the DSO, could provide a platform for transparent energy trans-

actions between different market entities that are not normally able to trade energy on the wholesale market [9]. Several recent studies have been carried out in this regard such as, for example, those presented in [1], [9]-[12] and [14]-[16].

In [1], the strategic behavior of a DSO in wholesale *dispatch* and *reserve* markets is modeled as a bi-level optimization problem and the Karush–Kuhn–Tucker (KKT) conditions and Duality theory are used to solve the proposed problem. In [9], it is discussed that, as the capacity of a single electric vehicle is too small to directly participate in the distribution-level market, load serving entities aggregators have emerged and, therefore, it is essential and promising to establish an efficient distribution-level market.

A novel market-clearing model to facilitate *dispatch* and flexibility transactions through coordinating providers in both transmission and distribution networks is proposed in [10], where the *dispatch* and flexibility market-clearing problem is formulated as a bi-level optimization model and KKT conditions and the Duality theory are used to transform and solve the proposed nonlinear problem. In [11], the authors presented a DSO framework for wholesale and retail market participation of DERs aggregators, where a linearized unbalanced power flow is tailored to model operating constraints of the distribution grid with various aggregators.

A two-stage stochastic model for security-constrained market clearing is proposed in [12], where wind plants and storage systems as network assets and elastic demands were used, and the effect of specifications of storage systems on social welfare has been investigated by solving the proposed model through the CPLEX optimization package [13]. In [14], the stochastic joint *dispatch* and *reserve* market clearing considering DERs uncertainty is addressed, where the problem is formulated as a chance-constrained two-stage stochastic programming model that minimizes the expected DSO cost and it is solved through a sample average approximation algorithm.

In [15], a local electricity-heat integrated *dispatch* market clearing method is proposed, in which the equilibrium between the DSO and the TSO is modeled as a mixed-integer second-order programming problem and solved using KKT Conditions and Duality theory. A nested transactive electricity market methodology is presented in [16] for the effective utilization of demand-side flexibility of small-scale residential consumers, where the formulated two-stage optimization-based scheduling model is solved using the Baron optimization package in the general algebraic modeling system.

In Table I, in order to clarify the contributions of the proposal presented in this paper, its relevant features are compared to the aforementioned works. Note that all these features are met only by the proposal presented in this paper. For the sake of clarity, the main contributions are listed below:

- 1) The proposed approach provides solutions for the DGs *dispatch* and *reserve* scheduling problem through a market-based clearing approach, which are valid for all possible scenarios limited by the load demand interval bounds and DGs<sub>U</sub> uncertainties, i.e., by providing solutions that are valid for a range of alternatives defined

by the bounds of the interval parameters, rather than for a single scenario as in classical deterministic and static approaches.

- 2) A new mixed integer linear programming (MILP) formulation considering interval variables and parameters which contributes to improving the solution through conventional optimization solvers, where the DGs are represented by accurate operation models of the most common technologies used to connect them to the network, such as SGs and DFigs.
- 3) Through this proposal, it is possible to identify the underlying risks associated to the payment burden of the DSO considering the uncertainties of the DGs<sub>U</sub> generation. In other words, by comparing the cases in which DGs<sub>U</sub> are participating with those in which this kind of generators is not considered, the percentage of risk associated with the solution provided by the proposed MCA can be clearly identified.
- 4) The proposed methodology facilitates a strategic DGs scheduling in which the DSO is able to be aware of critical scenarios imposed by the volatility of the load demand and DGs<sub>U</sub>.

TABLE I: Comparison with some recent researches on distribution system market clearing

Ref.	DG model		Market		Uncertainty		Type of DG		Risk analysis
	Det	Approx	Disp	Res	Dem	Gen	DG <sub>U</sub>	DG <sub>NU</sub>	
[1]	×	✓	✓	✓	×	✓	✓	×	×
[9]	×	✓	✓	✓	×	✓	✓	×	×
[10]	×	✓	✓	×	×	×	×	✓	×
[11]	×	✓	✓	✓	×	✓	✓	✓	×
[12]	×	✓	✓	×	×	✓	✓	✓	×
[14]	×	✓	✓	✓	×	✓	✓	✓	×
[15]	×	✓	✓	×	×	×	✓	×	×
[16]	×	✓	✓	×	×	✓	✓	✓	×
This paper	✓	×	✓	✓	✓	✓	✓	✓	✓

✓: Yes; ×: No; Det: Detailed; Approx: Approximated; *Disp*: *Dispatch*; *Res*: *Reserve*; Dem: Demand; Gen: Generation; DGs<sub>NU</sub>: DGs with non-uncertainties.

### C. Paper Organization

The remainder of this paper is structured as follows: the assumptions and proposed mathematical formulation of the interval co-optimization market-based problem are presented in Section II; the proposed MCA is detailed in Section III; the results and a discussion about several performed test are presented in Section IV; and, finally, the conclusions are detailed in Section V.

## II. ASSUMPTIONS AND MATHEMATICAL FORMULATION OF THE INTERVAL CO-OPTIMIZATION MARKET-BASED PROBLEM

The assumptions and mathematical formulation of the proposed problem are presented in next subsections.

### A. Assumptions

As noted above, a distribution-level market managed by the DSO provides a platform for those small market entities that are not normally eligible to participate in the wholesale electricity market [9]. In this context, *reserve* supply could

be accomplished via a coordinated approach through a central controller or, on the other hand, via an uncoordinated approach, where the controller for each DG is tuned with a predefined droop characteristic so that it can react to system frequency changes accordingly [17]. This setup works well for *reserve* markets that have a long-term contract (days, weeks, or even months) with a fixed amount of capacity reserved. In such markets, the DSO gets a fixed capacity contract from the TSO for a certain period and works out the optimal amount to be subcontracted to each DG, as shown in Fig. 1. In the proposal presented in this paper, where an uncoordinated approach is adopted, the *dispatch* and *reserve* markets coexist in a co-optimization structure in a day-ahead time basis.

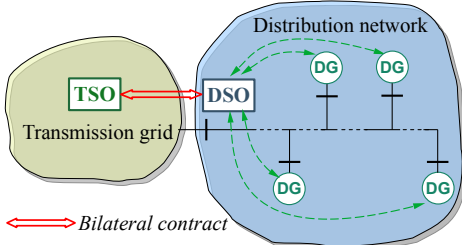


Fig. 1: Uncoordinated approach

In order to develop the mathematical formulation of the proposed interval co-optimization market-based problem, some assumptions were made, as presented below:

- 1) Since this approach is directed to primary distribution networks, the distribution system is balanced and represented by a monophasic equivalent.
- 2) In branch  $ij$ , node  $i$  is closer to the substation node than node  $j$  and the active and reactive power losses are concentrated in node  $i$ .
- 3) The market-clearing problem is solved from the stand point of the DSO; therefore, *dispatch* and *reserve* are purchased from all the participating DGs by a single buyer, the DSO, which performs the market clearing. The DSO can also buy active power from the main grid.
- 4) The offers of the DGs are presented such that the market is solved in a day-ahead basis. These offers consist of prices and capacities of *dispatch* and *reserve*.
- 5) All DGs providing *dispatch* and/or *reserve* are paid based on the interval *dispatch* locational marginal prices (DLMPs $^\pm$ ) and the interval *reserve* marginal prices (RMP $^\pm$ ).
- 6) The definition of the interval number  $H^\pm = [H^-, H^+]$ , for example, means that  $H$  could take values between bounds  $H^-$  and  $H^+$ . Additionally,  $H^\pm$  has width, middle, uncertainty degree and expected values ( $W[H^\pm]$ ,  $M[H^\pm]$ ,  $U[H^\pm]$  and  $EV[H^\pm]$ , respectively).

### B. Mathematical Formulation of the Interval Co-optimization Market-based Problem

The co-optimization market-based problem formulated in this work corresponds to an interval MILP problem, which consists of the objective function (1), subject to the set of constraints (2)-(25).

$$\text{Min } PB^\pm = \sum_{t \in \Omega_T} \sum_{i \in \Omega_{\text{Bus}}} \left( \alpha_t P_{SS,i,t}^\pm + \sum_{g \in \Omega_{\text{DG}}} (o f_{E,g,t} E_{g,i,t}^\pm + f r_{g,t} R_{g,i,t}^\pm) \right) \quad (1)$$

Subject to:

$$\sum_{ij \in \Omega_{\text{UBr}}} P_{ij,t}^\pm - \sum_{ij \in \Omega_{\text{DBr}}} (P_{ij,t}^\pm + R_{\text{Br},ij} \text{I}_{ij,t}^{\text{Sq}\pm}) + P_{SS,i,t}^\pm + \sum_{g \in \Omega_{\text{DG}}} E_{g,i,t}^\pm = P_{D,i,t}^\pm \quad (2)$$

$$\sum_{ij \in \Omega_{\text{UBr}}} Q_{ij,t}^\pm - \sum_{ij \in \Omega_{\text{DBr}}} (Q_{ij,t}^\pm + X_{\text{Br},ij} \text{I}_{ij,t}^{\text{Sq}\pm}) + Q_{SS,i,t}^\pm + \sum_{g \in \Omega_{\text{DG}}} Q_{g,i,t}^\pm = Q_{D,i,t}^\pm \quad (3)$$

$$V_{i,t}^{\text{Sq}\pm} - 2(R_{\text{Br},ij} P_{ij,t}^\pm + X_{\text{Br},ij} Q_{ij,t}^\pm) - \bar{Z}_{\text{Br},ij}^2 \text{I}_{ij,t}^{\text{Sq}\pm} - V_{j,t}^{\text{Sq}\pm} = 0 \quad (4)$$

$$\underline{V}^2 + \sum_{u \in \Omega_{\text{Disc}}} (\pi_{\bar{V},u,j,t}^\pm \bar{\Delta}V) \leq V_{j,t}^{\text{Sq}\pm} \leq \bar{V}^2 + \bar{\Delta}V + \sum_{u \in \Omega_{\text{Disc}}} (\pi_{\bar{V},u,j,t}^\pm \bar{\Delta}V) \quad (5)$$

$$\pi_{\bar{V},u^*-1,j,t}^\pm \leq \pi_{\bar{V},u^*,j,t}^\pm \quad (6)$$

$$0 \leq \bar{\Delta}V \text{I}_{ij,t}^{\text{Sq}\pm} - P_{C,u,j,t}^\pm \leq \bar{\Delta}V \bar{I}_{ij}^2 (1 - \pi_{\bar{V},u,j,t}^\pm) \quad (7)$$

$$0 \leq P_{C,u,j,t}^\pm \leq \bar{\Delta}V \bar{I}_{ij}^2 \pi_{\bar{V},u,j,t}^\pm \quad (8)$$

$$P_{ij,t}^{\uparrow\pm} - P_{ij,t}^{\downarrow\pm} = P_{ij,t}^\pm \quad (9)$$

$$Q_{ij,t}^{\uparrow\pm} - Q_{ij,t}^{\downarrow\pm} = Q_{ij,t}^\pm \quad (10)$$

$$P_{ij,t}^{\uparrow\pm} + P_{ij,t}^{\downarrow\pm} = \sum_{l \in \Omega_L} \Delta_{P,l,ij,t}^\pm \quad (11)$$

$$Q_{ij,t}^{\uparrow\pm} + Q_{ij,t}^{\downarrow\pm} = \sum_{l \in \Omega_L} \Delta_{Q,l,ij,t}^\pm \quad (12)$$

$$0 \leq \Delta_{P,l,ij,t}^\pm \leq \bar{\Delta}S_{ij} \quad (13)$$

$$0 \leq \Delta_{Q,l,ij,t}^\pm \leq \bar{\Delta}S_{ij} \quad (14)$$

$$0 \leq P_{ij,t}^{\uparrow\pm}, P_{ij,t}^{\downarrow\pm}, Q_{ij,t}^{\uparrow\pm}, Q_{ij,t}^{\downarrow\pm} \quad (15)$$

$$\left( \bar{V}^2 + \frac{\bar{\Delta}V}{2} \right) \text{I}_{ij,t}^{\text{Sq}\pm} + \sum_{u \in \Omega_{\text{Disc}}} P_{C,u,j,t}^\pm = \sum_{l \in \Omega_L} m_{S,l,ij} (\Delta_{P,l,ij,t}^\pm + \Delta_{Q,l,ij,t}^\pm) \quad (16)$$

$$\sum_{i \in \Omega_{\text{Bus}}} \sum_{g \in \Omega_{\text{DG}}} R_{g,i,t}^\pm = R_{\text{Req},t}^\pm \quad (17)$$

$$\frac{E_{g,i,t}^\pm + R_{g,i,t}^\pm}{Q_{\text{DG},g,i,t}^\pm} \leq \frac{P_{1,g}}{Q_{1,g}} \quad (18)$$

$$\frac{E_{g,i,t}^\pm + R_{g,i,t}^\pm - P_{h,g}}{Q_{\text{DG},g,i,t}^\pm - Q_{h,g}} \leq \frac{P_{h,g} - P_{h-1,g}}{Q_{h,g} - Q_{h-1,g}}; \quad \forall h \in \{2, 3, 4\} \quad (19)$$

$$\frac{E_{g,i,t}^\pm + R_{g,i,t}^\pm}{Q_{\text{DG},g,i,t}^\pm - Q_{\text{DG},g}^\pm} \leq \frac{P_{4,g}}{Q_{4,g} - Q_{\text{DG}}^\pm} \quad (20)$$

$$0 \leq E_{g,i,t}^\pm + R_{g,i,t}^\pm \leq \bar{P}_{\text{DG},g,t}^\pm \quad (21)$$

$$E_{g,i,t}^\pm \geq 0 \quad (22)$$

$$R_{g,i,t}^\pm \geq 0 \quad (23)$$

$$\underline{V}^2 \leq V_{i,t}^{\text{Sq}\pm} \leq \bar{V}^2 \quad (24)$$

$$0 \leq \text{I}_{ij,t}^{\text{Sq}\pm} \leq \bar{I}_{ij}^2 \quad (25)$$

The objective function (1) is composed of three elements: the costs of active power bought from the main grid (provided at the grid supply point), i.e.,  $\sum_{t \in \Omega_T} \sum_{i \in \Omega_{\text{Bus}}} \alpha_t P_{SS,i,t}^\pm$ ; the costs for *dispatch* and *reserve* provided by the DGs, say  $FC^\pm$  in (26);

and the financial reward of the DSO for *reserve* sold to the main grid, say  $FR^\pm$  in (27). In (1), note that  $fr_{g,t} = of_{R,g,t} - \beta_t$ .

$$FC^\pm = \sum_{t \in \Omega_T} \sum_{i \in \Omega_{\text{Bus}g} \in \Omega_{\text{DG}}} \left( of_{E,g,t} E_{g,i,t}^\pm + of_{R,g,t} R_{g,i,t}^\pm \right) \quad (26)$$

$$FR^\pm = \sum_{t \in \Omega_T} \sum_{i \in \Omega_{\text{Bus}g} \in \Omega_{\text{DG}}} \left( \beta_t R_{g,i,t}^\pm \right) \quad (27)$$

The constraints that represent the steady-state operation of a radial distribution system correspond to expressions (2)-(16), which are commonly used in the load flow sweep method [18]. Constraints (2) and (3) are the conventional representation of the active and reactive power balance; while, through (4) and the linearized expressions (5)-(16), which were proposed in [19], it is possible to obtain the voltage of a final node  $j$  and the current in corresponding branch  $ij$ . It is worth noting that the linearized expressions (5)-(16) provide highly accurate results, as discussed in detail in [19]. In (17), the required *reserve* to be met by the DGs is represented. Constraints (18)-(22) represent the DGs operational limits, which are linear expressions related to the capability curves of the SGs and DFIGs, as presented in [19]. Constraint (23) represents the *reserve* non-negativity condition. Node voltages must be within the specified limits, according to (24), and currents through branches must be less than the specified maximum values, as shown in (25).

The interval optimization problem presented before is very difficult to be solved due to its MILP nature and additional computational burden introduced by its interval characteristics. Therefore, in this work, Benders decomposition is implemented to decompose the original interval problem into an EMP and an IFChS according to the proposed MCA presented in Section III. It is remarkable that, before applying the MCA, the bounds of the interval parameters corresponding to the load demand and generation limits of the DGs<sub>U</sub> need to be defined; therefore, two probabilistic load demand bounds scenarios (LDBSs) and two wind speed bounds scenarios (WSBSs) are defined through an EFS-RT based on the forecasting methodology proposed in [7].

### III. PRICING OF DISPATCH AND RESERVE

In order to price *dispatch* and *reserve*, the DLMPs $^\pm$  are defined based on the dual variables of the active power balance constraints (2), say  $\lambda_{E,g,i,t}^\pm$ , and the RMP $^\pm$  is defined based on the dual variable of the *reserve* constraint (17), say  $\lambda_{R,g,i,t}^\pm$ . These market prices are defined by using Benders decomposition and scenario reduction based on ILP theory in the proposed MCA. Thus, the interval co-optimization market-based problem is decomposed into an EMP, which is evaluated under the expected values, and an IFChS, which is evaluated under interval values. This decomposition, as well as the MCA, are presented in next subsections.

#### A. Expected Master Problem

The EMP is defined as the minimization of the objective function (1), subject to the set of constraints (2)-(25) evaluated at the expected values conditions, and including the set of

Benders cuts [5], which grant feasibility in other possible states defined by the load demand interval values.

The solution of the EMP brings the results of the co-optimization market-based problem under expected values conditions and, in order to check the feasibility of this solution in other possible states, the feasibility under load demand interval values is checked by solving the IFChS. Then, the corresponding cuts, if needed, are returned back from the IFChS to the EMP to improve the feasibility of the entire problem. While the EMP can be solved by using any MILP optimization technique, the IFChS needs an in-depth analysis in order to reduce the large amount of load demand states generated by the interval characteristic of this parameter.

#### B. Interval Values Feasibility Check Sub-problem

The interval values dependent constraints impose the need of evaluating a set of numerous possible system states (defined according to all possible load demand states inside the limits of their corresponding interval values), which cannot be solved directly. Therefore, the purpose in the solution of the IFChS is to find out some representative critical states, which are called in this paper as pessimistic and optimistic states, and get the feasible solution for all possible states inside these limits by only checking these critical ones instead. These critical states are identified in this paper by using the ILP theory [6].

The IFChS is defined as the ILP problem (28)-(34), where constraints (29)-(32) are presented in a compact form with the aim of facilitating the analysis of all possible load demand states between the limits defined by their interval values. Any violation of the IFChS constraints indicates that the corresponding solutions brought by the EMP cannot satisfy the operation requirement at some certain load demand state. Then, according to the Benders decomposition theory, the corresponding Benders cuts are generated and returned back to the EMP.

$$\text{Min } \nu = \sum_{t \in \Omega_T} \sum_{st \in \Omega_{st}} \left( \sum_{i \in \Omega_{\text{Bus}}} \left( \lambda_{B,1,i,t}^{P(st)} + \lambda_{\text{Bal},2,i,t}^{P(st)} + \lambda_{B,1,i,t}^{Q(st)} + \lambda_{\text{Bal},2,i,t}^{Q(st)} \right) + \sum_{q \in \Omega_{\text{In}}^P} \left( \lambda_{\text{In},1,q,t}^{P(st)} + \lambda_{\text{In},2,q,t}^{P(st)} \right) + \sum_{q \in \Omega_{\text{In}}^Q} \left( \lambda_{\text{In},1,q,t}^{Q(st)} + \lambda_{\text{In},2,q,t}^{Q(st)} \right) \right) \quad (28)$$

Subject to:

$$\Psi_{B,i,t}^{P,(st)}(\cdot) + \lambda_{B,1,i,t}^{P(st)} - \lambda_{B,2,i,t}^{P(st)} = 0 \quad (29)$$

$$\Psi_{B,i,t}^{Q,(st)}(\cdot) + \lambda_{B,1,i,t}^{Q(st)} - \lambda_{B,2,i,t}^{Q(st)} = 0 \quad (30)$$

$$\underline{\Psi}_{\text{In},i,q,t}^{P,(st)} \leq \Psi_{\text{In},i,q,t}^{P,(st)}(\cdot) + \lambda_{\text{In},1,i,q,t}^{P(st)} + \lambda_{\text{In},2,i,q,t}^{P(st)} \leq \overline{\Psi}_{\text{In},i,q,t}^{P,(st)} \quad (31)$$

$$\underline{\Psi}_{\text{In},i,q,t}^{Q,(st)} \leq \Psi_{\text{In},i,q,t}^{Q,(st)}(\cdot) + \lambda_{\text{In},1,i,q,t}^{Q(st)} + \lambda_{\text{In},2,i,q,t}^{Q(st)} \leq \overline{\Psi}_{\text{In},i,q,t}^{Q,(st)} \quad (32)$$

$$\lambda_{B,1,i,t}^{P(st)}, \lambda_{B,2,i,t}^{P(st)}, \lambda_{\text{In},1,q,t}^{P(st)}, \lambda_{\text{In},2,q,t}^{P(st)} \geq 0 \quad (33)$$

$$\lambda_{B,1,i,t}^{Q(st)}, \lambda_{B,2,i,t}^{Q(st)}, \lambda_{\text{In},1,q,t}^{Q(st)}, \lambda_{\text{In},2,q,t}^{Q(st)} \geq 0 \quad (34)$$

The  $\lambda$ -variables in (28) are non-negative slack variables, which are added to guarantee the feasibility of the IFChS. A positive value of  $\nu$  in (28) means that the solutions of the EMP

cannot satisfy all possible load demand conditions within the limits specified by their corresponding interval values.

Initially, an analysis of the interval values dependent constraints associated to the active and reactive power demand (29)-(32) needs to be carried out in order to define the pessimistic and optimistic states. According to [6], it is possible to define the pessimistic state when constraints (29)-(32) reach their lower limits. In contrast, the optimistic state is defined when these constraints reach their upper limits. Note that the pessimistic and optimistic states represent, respectively, the tightest and laxest constraints under all possible states.

For the extreme conditions, i.e., for the pessimistic and optimistic states, there is a considerably large amount of  $2^{|\Omega_T|}$  possible states (i.e., when a number of  $|\Omega_T|$  time intervals is considered). However, taking advantage of the fact that the constraints of each time interval of the IFChS are only associated to the power generation at the same time interval, only a reduced set of  $2 \times |\Omega_T|$  states need to be formulated. An in-depth analysis in this regard is available in [6].

It is noteworthy that the above procedure significantly reduces the number of cases that need to be analyzed in the IFChS. Consequently, the initial IFChS with various possible states is transformed into a much less difficult IFChS with a reasonable number of constraints, improving the tractability and efficiency of the MCA, which is proposed in Subsection III-C.

### C. Co-optimization Market-based Clearing Algorithm

In this paper, the MCA is proposed as a combination of the concepts that have been presented so far in this section, as shown below:

- Step 1. Inputs: Total number of hours  $|\Omega_T|$  and interval parameters LDBSs and WSBSs, which are defined through the EFS-RT [7].
- Step 2. Set  $k \leftarrow 0$ .
- Step 3. Solve the EMP (Subsection III-A).
- Step 4. Solve the IFChS (Subsection III-B). When solving the IFChS, define which load demand bound yields to the pessimistic state and which one yields to the optimistic state.
- Step 5. If the objective function of the IFChS (28) is positive, then generate the corresponding Benders feasibility cuts and go to Step 6; otherwise, i.e., if the objective function of the IFChS is zero, then go to Step 7.
- Step 6. Set  $k \leftarrow k + 1$  and go to Step 3.
- Step 7. Output: Interval market clearing prices of *dispatch* and *reserve*.

In order to clarify the proposal presented in this paper, a flowchart summarizing the entire market clearing process, beginning from the EFS-RT, is presented in Fig. 2. It is worth noting that the MCA is essentially independent of the EFS-RT, which means that the process of defining the bounds of the interval parameters, which are required to begin the solution process through the MCA, can be done by any other probabilistic scenarios generation methodology. This versatility

feature of the MCA is subject of discussion in Subsection IV-B (Comparative Analysis). A detailed discussion of the market-based clearing approach proposed in this paper is presented in Section IV.

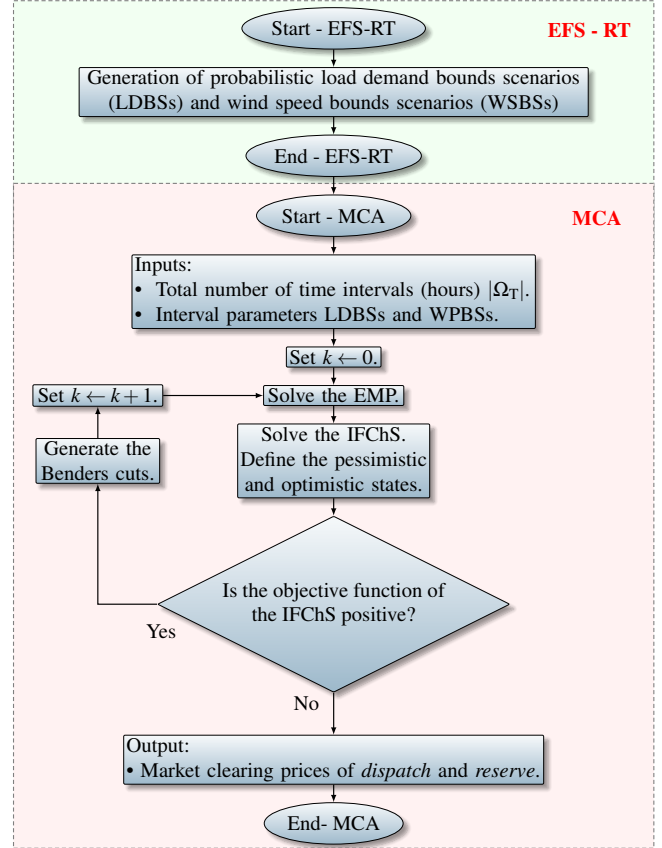


Fig. 2: Proposed market clearing process

## IV. RESULTS AND DISCUSSION

In this work, the implementations to solve the proposed problem were developed in AMPL (Algebraic Modeling Programming Language) [22], using the CPLEX optimization package [13], and the programming language C++ with the compiler g++ 4.4, in the Linux environment.

Tests of the proposed methodology were performed using data of the IEEE 37-bus distribution test system [8]. There were assumed five DGs as participants in the co-optimization market: three  $DG_{S_{NU}}$  (DGs with non-uncertainties, e.g., small hydro), coupled to the network through SGs, installed at nodes 714 ( $DG_1$ ), 727 ( $DG_2$ ) and 733 ( $DG_3$ ); and two  $DG_{S_U}$  (wind turbines), coupled to the network through DFIGs, installed at nodes 731 ( $DG_4$ ) and 738 ( $DG_5$ ).

For all tests, the overcurrent limit in branches was assumed as 200 A, the minimum and maximum node voltages limits were supposed as 0.95 and 1.05 pu, respectively, and the *reserve* requirement was fixed as 325 kW. Regarding the linearization parameters in the EMP formulation, the following values were used:  $\Omega_{Disc} = \{1, 2, \dots, 20\}$  and  $\Omega_L = \{1, 2, \dots, 30\}$ .

The daily load demand curve and the  $DG_{S_U}$  maximum active power generation limits presented in Figs. 3 and 4, respectively, were obtained through the EFS-RT [7].

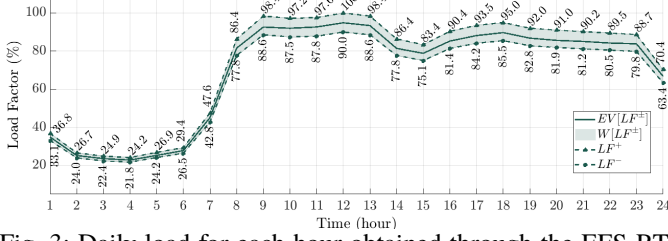


Fig. 3: Daily load for each hour obtained through the EFS-RT

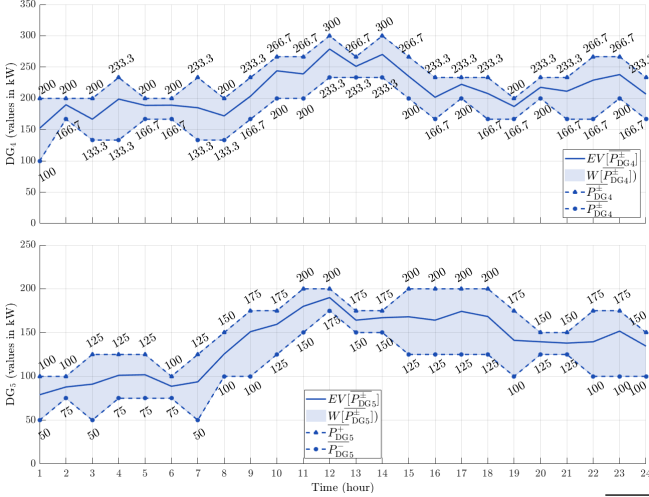


Fig. 4:  $DG_U$  maximum active power generation limits ( $P_{DG}^{\pm}$ ) obtained through the EFS-RT

Supposed expected values of offers of *dispatch* and *reserve* presented by the DGs, costs of *dispatch* purchased from the main grid by the DSO, and prices of *reserve* sold to the main grid by the DSO are shown in Table II.

#### A. Results of the Proposed MCA

The results of  $PB^{\pm}$ ,  $FC^{\pm}$ ,  $FR^{\pm}$ ,  $P_L^{\pm}$ , and the total active power provided by the substation and the DGs, say  $\hat{P}_{SS_T}^{\pm}$  and  $\hat{P}_{DG_T}^{\pm}$ , respectively, are presented in Table III. From the stand point of the DSO, the lower extreme result regarding the payment burden corresponds to the most optimistic benefit to the DSO with the highest risk of violating the constrains of the problem, while the higher extreme result represents the most pessimistic benefit to the DSO with the lowest risk. The financial compensation to the DGs for *dispatch* and *reserve* sold to the DSO (i.e.,  $FC^{\pm} = [2,107.89, 2,181.39]$  US\$) is slightly smaller in the most optimistic state (2,107.89 US\$) in 3.37% than in the most pessimistic one (2,181.39 US\$). Although the financial reward of the DSO for *reserve* sold to the main grid (i.e.,  $FR^{\pm} = [127.57, 264.15]$  US\$) is greater in the most pessimistic state (264.15 US\$) than in the most optimistic one (127.57 US\$), the liquid payment of the DSO (i.e.,  $PB^{\pm} - FR^{\pm} = [2,869.22, 3,729.84]$  US\$) remains as the worst in the most pessimistic state (3,729.84 US\$). The expected values of the market-clearing prices obtained through this proposal are presented in Table IV.

The values of  $PB^{\pm}$  for each hour of the day with their corresponding uncertainties, i.e.,  $U[PB^{\pm}]$  (represented by the

TABLE II: Expected values of offers presented by DGs, costs and prices of *reserve* for the DSO ( $10^{-2}$  US\$/kWh)

t	$o_{E,1,t}^{\pm}$	$o_{R,1,t}^{\pm}$	$o_{E,2,t}^{\pm}$	$o_{R,2,t}^{\pm}$	$o_{E,3,t}^{\pm}$	$o_{R,3,t}^{\pm}$	$o_{E,4,t}^{\pm}$	$o_{R,4,t}^{\pm}$	$o_{E,5,t}^{\pm}$	$o_{R,5,t}^{\pm}$	$\alpha_t^{\pm}$	$\beta_t^{\pm}$
1	8.90	3.00	8.90	3.00	8.90	3.10	8.90	3.90	8.90	1.80	11.80	6.00
2	7.50	1.80	7.50	2.30	7.50	1.80	7.50	1.80	7.60	3.40	9.90	4.50
3	6.70	2.80	6.60	1.60	6.70	2.20	6.60	1.80	6.70	1.90	9.80	3.70
4	6.80	3.00	6.80	2.60	6.80	2.00	6.70	2.00	6.70	2.10	9.50	4.70
5	7.40	2.10	7.40	2.00	7.40	2.50	7.30	3.50	7.20	2.60	9.70	4.20
6	6.70	3.40	6.70	3.10	6.80	2.30	6.60	2.30	6.70	2.40	10.60	5.10
7	10.00	2.70	10.00	3.00	10.00	3.60	9.90	1.40	9.90	3.10	12.60	5.90
8	11.50	5.20	11.40	6.00	11.50	6.00	11.60	4.40	11.40	3.10	14.50	7.60
9	12.10	2.80	12.10	2.80	12.10	3.70	12.00	4.20	12.10	3.30	14.50	7.80
10	11.60	4.20	11.50	3.90	11.60	4.20	11.40	2.80	11.50	3.80	14.20	7.60
11	11.60	2.70	11.60	3.40	11.60	4.00	11.50	2.10	11.60	3.90	14.20	8.10
12	10.80	4.80	10.70	4.20	10.80	6.20	10.50	3.40	10.60	4.60	14.30	7.80
13	10.70	4.30	10.80	4.50	10.80	4.90	10.60	3.60	10.70	3.70	13.80	7.60
14	12.90	2.30	13.00	2.60	13.20	1.40	12.80	4.10	12.90	4.00	13.70	7.80
15	12.10	3.80	12.10	4.20	12.20	2.70	11.90	2.70	12.00	4.20	13.90	7.70
16	11.20	3.00	11.20	3.50	11.30	3.60	11.10	2.20	11.20	4.00	13.60	7.70
17	11.40	3.70	11.30	4.30	11.40	4.60	11.30	3.00	11.30	3.60	13.60	7.20
18	11.30	4.40	11.30	3.60	11.40	5.10	11.30	4.70	11.20	3.80	14.80	7.70
19	11.20	3.30	11.20	3.20	11.30	4.10	11.30	3.50	11.30	3.60	14.10	7.50
20	10.80	4.10	10.70	4.40	10.70	5.50	10.60	4.10	10.70	4.00	13.70	7.80
21	11.80	4.90	11.80	3.90	11.90	4.10	11.70	2.10	11.70	4.00	14.50	7.50
22	11.40	6.00	11.50	6.00	11.70	5.90	11.40	5.40	11.50	4.80	13.60	8.30
23	11.90	4.00	11.90	3.50	12.10	3.60	11.90	4.70	12.00	3.90	14.60	7.80
24	12.30	2.10	12.30	2.00	12.40	1.90	12.10	3.30	12.20	3.80	14.00	7.00

TABLE III: Results of the MCA

Result	Interval value	Expected value
$PB^{\pm}$ (US\$)	[2,996.79, 3,993.99]	3,598.95
$FC^{\pm}$ (US\$)	[2,107.89, 2,181.39]	2,154.19
$FR^{\pm}$ (US\$)	[127.57, 264.15]	197.23
$P_L^{\pm}$ (kW)	[257.33, 327.74]	304.50
$\hat{P}_{SS_T}^{\pm}$ (kW)	[10,387.49, 13,193.80]	12,323.84
$\hat{P}_{DG_T}^{\pm}$ (kW)	[20,852.58, 22,933.00]	22,184.05

TABLE IV: Expected values of the market-clearing prices of *dispatch* and *reserve* ( $10^{-2}$ US\$/kWh)

t	$\xi_{E,1,t}^{\pm}$	$\xi_{R,1,t}^{\pm}$	$\xi_{E,2,t}^{\pm}$	$\xi_{R,2,t}^{\pm}$	$\xi_{E,3,t}^{\pm}$	$\xi_{R,3,t}^{\pm}$	$\xi_{E,4,t}^{\pm}$	$\xi_{R,4,t}^{\pm}$	$\xi_{E,5,t}^{\pm}$	$\xi_{R,5,t}^{\pm}$
1	8.92	3.07	8.87	2.97	8.92	2.98	8.88	3.87	8.93	1.76
2	7.60	1.76	7.60	2.25	7.49	1.80	7.51	1.75	7.38	3.35
3	6.68	2.67	6.65	1.55	6.74	2.18	6.71	1.82	6.67	1.88
4	6.69	2.91	6.75	2.58	6.76	1.99	6.79	1.97	6.70	2.11
5	7.36	2.12	7.31	2.00	7.43	2.50	7.23	3.42	7.21	2.60
6	6.78	3.51	6.65	3.10	6.84	2.32	6.64	2.30	6.77	2.38
7	9.94	2.71	9.93	3.10	10.14	3.23	10.00	1.43	9.99	3.20
8	11.47	5.57	11.43	5.94	11.51	6.29	11.49	4.38	11.47	3.30
9	12.15	2.82	12.03	2.78	12.15	3.55	11.99	4.20	12.21	3.28
10	11.56	4.25	11.46	4.00	11.63	4.16	11.42	2.70	11.46	3.78
11	11.53	2.79	11.61	3.42	11.64	3.78	11.50	2.13	11.57	3.91
12	10.73	4.71	10.75	4.13	10.84	6.24	10.48	3.26	10.57	4.53
13	10.67	4.36	10.70	4.53	10.84	4.90	10.58	3.57	10.64	3.79
14	12.99	2.23	13.05	2.63	13.00	1.47	12.73	4.08	12.72	3.94
15	12.07	3.83	12.07	4.25	12.17	2.71	11.93	2.65	11.99	4.08
16	11.16	2.95	11.19	3.52	11.27	3.60	11.07	2.16	11.18	3.86
17	11.39	3.42	11.31	4.27	11.40	4.41	11.27	3.00	11.27	3.57
18	11.29	4.37	11.33	3.68	11.44	4.85	11.23	4.59	11.29	3.83
19	11.21	3.55	11.19	3.17	11.30	3.91	11.23	3.56	11.28	3.59
20	10.74	4.07	10.72	4.23	10.83	5.08	10.67	4.09	10.58	4.03
21	11.69	4.77	11.74	3.86	11.85	4.12	11.60	2.18	11.68	3.97
22	11.44	6.11	11.49	6.03	11.70	5.37	11.48	5.40	11.42	4.91
23	11.98	3.98	11.94	3.55	12.06	3.47	11.88	4.56	11.98	3.93
24	12.31	2.19	12.27	2.02	12.34	2.04	12.16	3.24	12.23	3.79

radius of spheres at each time instant), are presented in Fig. 5. Note that the biggest uncertainties of  $PB^{\pm}$  occur in the first seven hours of the day, when the middle values of  $PB^{\pm}$  are the lowest, considering that the uncertainty degree of an interval variable is inversely proportional to its middle value. A low value of  $U[PB^{\pm}]$  means that its associated operating point has high probability to happen. As expected, in a normal operation of a distribution network, and as it was assumed in this work, medium and nominal load demand values (assumed here as values greater than 50% in Fig. 3) are more common (as shown in Fig. 5); consequently, the maximum costs, associated to these demand values, are also more likely to happen.

The active power generation of all DGs and that provided by the substation are presented in Fig. 6. In this figure, as it

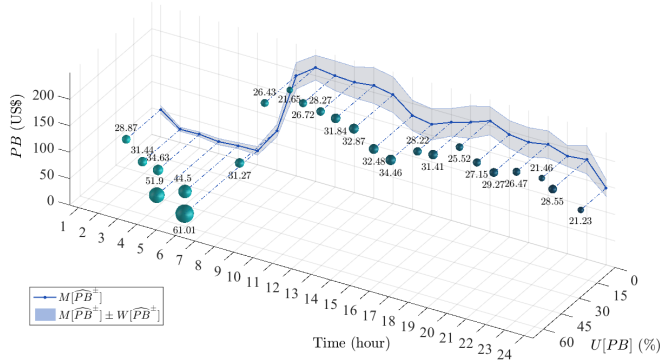


Fig. 5:  $PB^\pm$  for all hours of the day

was already presented in Table III, note that the participation of the DGs generating active power (with both *dispatch* and *reserve*) is bigger than the participation of the substation (only with *dispatch*).

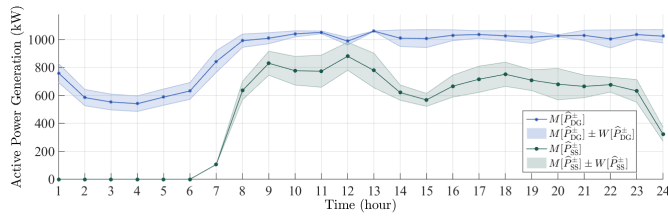


Fig. 6: Substation and DGs active power generation

The participation of each DG generating active power is presented in Fig. 7. In this figure, note that DG<sub>2</sub> is the generator with the greatest participation, since it is at full capacity almost all the time. Note also that the maximum variations in generation occur in DG<sub>4</sub> and DG<sub>5</sub>, which is expected, as these are the wind generators, which introduce the greatest variations in the results.

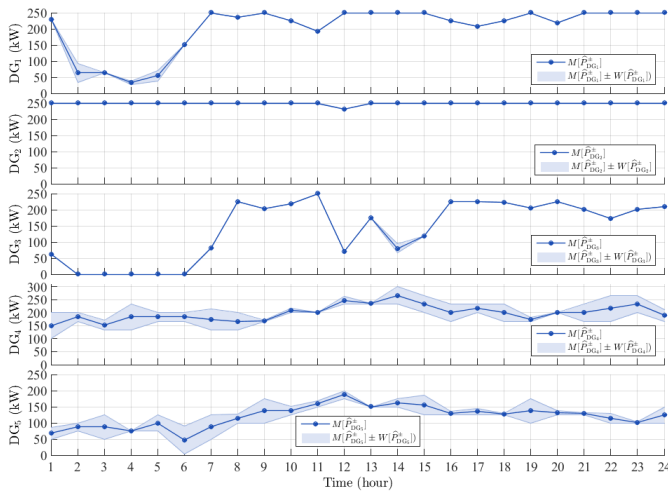


Fig. 7: Active power generated by the DGs

In order to perform a risk analysis of the payment burden of the DSO regarding the presence of DGs<sub>U</sub>, initially, it is assumed as reference case, or worst possible scenario, the one in which no DGs are installed in the network and there is no *reserve* requirement, which is compared to the case solved through the proposed MCA (considering all DGs and *reserve*

requirement). The risk associated to the results of  $PB^\pm$  is presented in Fig. 8, where the minimum and maximum risk values are 21.68% and 74.06%, and they occur at hours 6 and 10, respectively. Note that the higher risks are in the first hours of the day, when there is less participation of the DGs<sub>NU</sub> in the results of the MCA, as it can be confirmed in Fig. 7.

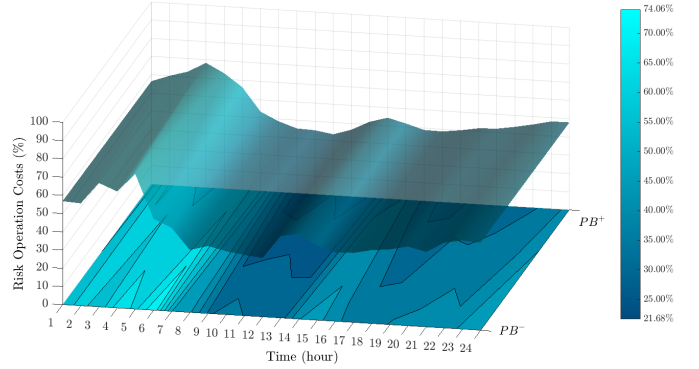


Fig. 8: Risk of the payment burden regarding the case with no DGs and no *reserve* requirement

Now, assuming as the reference case that in which only DGs<sub>NU</sub> are considered and there is *reserve* requirement, the corresponding risk associated to the results of the payment burden in the proposed MCA (considering all DGs and *reserve* requirement) is presented in Fig. 9. The minimum and maximum risk values in Fig. 9 are 3.38% and 40.20%, and they occur at hours 4 and 24, respectively. Again, the higher risks are in the first hours of the day, when there is less participation of the DGs<sub>NU</sub>; however, the maximum risk decreases in 47.72% regarding the case in which there are no DGs and no *reserve* is required (Fig. 8). In these studied cases, when there are more market participants, the risk associated to the payment burden decreases, which confirms the behavior expected in a competitive market.

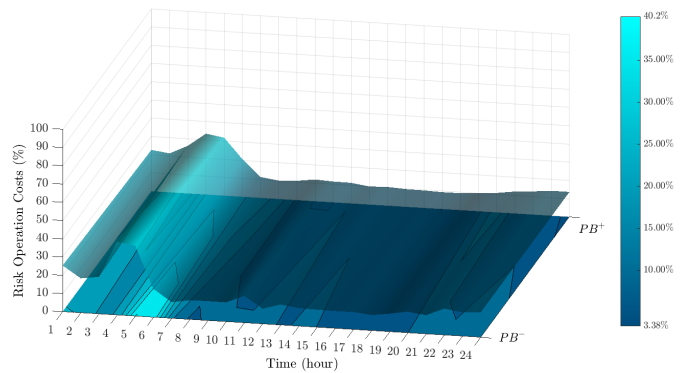


Fig. 9: Risk of the payment burden regarding the case with only DGs<sub>NU</sub> and with *reserve* requirement

### B. Comparative Analysis

As highlighted previously, one of the main advantages of the MCA proposed in this work is the ability to incorporate interval-numbers uncertainties into the linear model without any assumption of probability distributions. In this subsection,



in order to clarify this advantage, comparative analyzes are presented including the MCA and two methods: *i*) a scenario-based probability distributions approach (SPDA), in which a large number scenarios need to be generated in order to simulate the possible uncertainties; and, *ii*) a combination of the proposed MCA and probability distributions, which has been named in this paper as hybrid method (MCA-Hybrid).

In the SPDA, a large number of 50,000 scenarios was generated to simulate wind speed and load demand uncertainties. In this work, for the SPDA, the Weibull probability distribution function was used to simulate the wind speed [20], while the normal probability distribution was used to simulate the load demand [21]. In the SPDA, the reduction methodology presented in [7] was used to obtain a total of 100 probabilistic scenarios. The application of this reduction methodology in the SPDA plays an important role, since it significantly reduces the computation burden in a method that already presents difficulties in this regard. However, as it is discussed in this subsection, this reduction in scenarios is not enough to make the SPDA competitive regarding the proposed MCA in terms of runtimes performance and robustness of the results.

The results of payment burden of the implemented SPDA are shown in Fig. 10, where these values are also compared to the analogous results obtained through the MCA. In this figure, note that there are 15 scenarios with payment burden greater than the one corresponding to  $PB^+$  (3993.99 US\$), found in the MCA solution. In the SPDA, the scenario with the maximum value of payment burden, which is 4,194.49 US\$, is 5.02% higher than the upper bound found in the MCA ( $PB^+$ ), while the expected value in the SPDA ( $PB^{(0)}$ ), which is 3,892.40 US\$, is 8.15% higher than the expected value found in the MCA ( $EV[PB^\pm]$ ), which is 3,598.95 US\$.

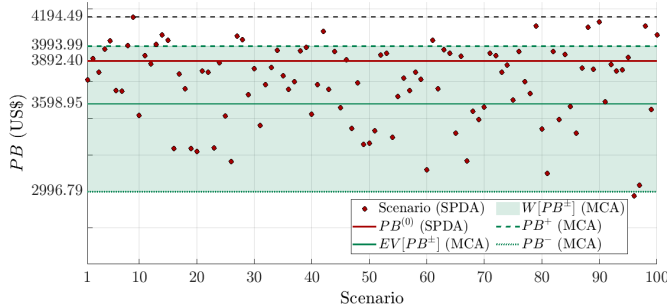


Fig. 10: Values of  $PB$  in the SPDA compared to those obtained in the proposed MCA.

In Table V, summarized results of the SPDA ( $PB^\pm$ ,  $FC^\pm$ ,  $FR^\pm$ ,  $P_L^\pm$ ,  $\hat{P}_{SS_T}^\pm$  and  $\hat{P}_{DG_T}^\pm$ ), as well as comparative percentages of these values in relation to the results of the proposed MCA (Table III) are presented. In this table, note that differences in percentages are between 4.53% and 8.15% above the reference values (MCA results). At this point, in this comparative analysis, it is clear that the SPDA brings results with higher values than those obtained with the MCA.

Another comparison made in this section relates to a version that combines the proposed MCA with probability distributions, which was called in this work as MCA-Hybrid.

In this hybrid version of the MCA, the solution process itself is exactly the same as defined in Section III (Pricing of *Dispatch* and *Reserve*), except that the scenarios for defining the bounds of the interval parameters are not generated using the EFS-RT (commented at the end of Subsection II-B), but using probability distributions for generating 10,000 probabilistic scenarios. The values of  $PB^\pm$ ,  $FC^\pm$ ,  $FR^\pm$ ,  $P_L^\pm$ ,  $\hat{P}_{SS_T}^\pm$  and  $\hat{P}_{DG_T}^\pm$  obtained through the MCA-Hybrid are presented in Table VI.

TABLE V: Results of the SPDA

Result	Max., min. values	Expected value	Comparative percentage
$PB^\pm$ (US\$)	2,970.03, 4,194.49	3,892.40	108.15
$FC^\pm$ (US\$)	1,691.00, 2,605.05	2,251.69	104.53
$FR^\pm$ (US\$)	127.57, 264.15	210.88	106.92
$P_L^\pm$ (kW)	264.36, 382.74	323.57	106.26
$\hat{P}_{SS_T}^\pm$ (kW)	9,547.81, 13,691.11	13,175.22	106.91
$\hat{P}_{DG_T}^\pm$ (kW)	19,353.88, 25,625.14	23,379.35	105.39

TABLE VI: Results of the MCA-Hybrid

Result	Interval value	Expected value
$PB^\pm$ (US\$)	[3,006.01, 4,223.85]	3,861.72
$FC^\pm$ (US\$)	[1,799.55, 2,513.53]	2,249.36
$FR^\pm$ (US\$)	[127.57, 264.15]	217.71
$P_L^\pm$ (kW)	[281.33, 369.30]	339.39
$\hat{P}_{SS_T}^\pm$ (kW)	[10,160.75, 13,210.15]	12,173.36
$\hat{P}_{DG_T}^\pm$ (kW)	[20,596.34, 24,724.95]	23,321.22

In Table VI, note that the results obtained with the MCA-Hybrid, similar to those obtained with the SPDA, are higher than the ones obtained with the proposed MCA. Nevertheless, the MCA-Hybrid could be an interesting option from the runtimes standpoint, since, as shown in Table VII, where runtimes for all cases are presented, the MCA-Hybrid is the method with the shortest runtime for the entire market clearing process (59.05 seconds). In Table VII, when comparing the MCA and MCA-Hybrid, the main decrease in runtime for the MCA-Hybrid is in the scenarios generation stage, which in this method is performed by using probability distributions. On the other hand, when the SPDA and MCA runtimes are compared, the SPDA take 9.17 times longer than the MCA.

TABLE VII: Runtimes in all cases (in seconds)

Process	SPDA	MCA	MCA-Hybrid
Scenarios generation	-	15.51	10.69
Market clearing	587.46	48.53	48.36
Total	587.46	65.05	59.05

Finally, considering as basis for the risk analysis the scenario where there is no DGs participation and no *reserve* is required, the expected values of the risk associated to the DGs active power generation in the MCA, MCA-Hybrid and SPDA are presented in Fig. 11. In this figure, note that the risk expected values in the SPDA and MCA-Hybrid are similar; this behavior is due to the fact that, mainly in the early hours of the day, the participation of DGs is greater in these cases than in the MCA, which can be confirmed by comparing tables III, V and VI, where the expected values of the DGs active power generation in the SPDA and MCA-Hybrid are, respectively, 5,39% and 5,13% above the analogous expected values in the MCA.

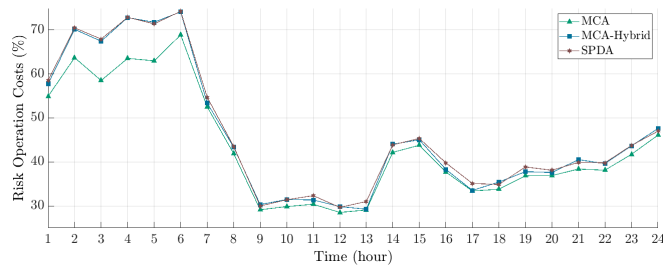


Fig. 11: Risk expected values of all cases regarding the case with no DGs and no reserve requirement

## V. CONCLUSIONS

In this paper, a novel methodology to solve the DGs *dispatch* and *reserve* scheduling problem in active power distribution networks in a co-optimization market-based environment was proposed. In this approach, uncertainties of load demand and DGs with high degree of variability are addressed through an MILP formulation with interval variables and parameters.

Through the proposed methodology, the problem can be solved efficiently using a conventional MILP solver. According to the results, the amount of DGs participating in the market influences the economic advantages to the DSO. When more DGs participate in the market, the payments of the DSO tend to decrease because less active power (at a higher cost) is bought from the main grid.

As in the proposal presented in this paper it is assumed an uncoordinated approach, in which the DSO gets a fixed *reserve* capacity contract from the TSO for a certain period, the DSO would not necessarily behave as an explicit neutral agent. However, as the financial reward ( $FR^\pm$ ) corresponds to a fixed contracted *reserve* with a fixed price, this result ([127.57, 264.15] US\$) is the same interval value in all implemented study cases; consequently, this term may or may not be used in the objective function at will, allowing the DSO to participate as a “neutral middle agent”, which transfers the corresponding payments to the DGs, or as a “profit-making aggregator”.

Comparative analyses show the efficiency of the proposed MCA regarding methods based on probability distributions. The MCA’s response speed proved to be faster than the SPDA by 9.17 times. The upper bound of the payment burden result provided by the MCA ( $PB^+$ ) is lower by around 95% regarding the payment burden of the most expensive scenario in the SPDA, while the payment burden expected value of the MCA ( $EV[PB^\pm]$ ) is around 92% of the payment burden expected value of the SPDA ( $PB^{(0)}$ ). In addition, the proposed MCA brings results with better confidence intervals, reducing the risks associated with the DSO’s decision-making process. The proposed MCA allows the DSO to be aware of the risks imposed by the volatility of the load demand and DGs<sub>U</sub> generation capabilities and encourages its participation in the wholesale electricity market.

## REFERENCES

[1] S. Bahramara, M. Yazdani-Damavandi, J. Contreras, M. Shafie-Khah and J. P. S. Catalao, *Modeling the Strategic Behavior of a Distribution*

*Company in Wholesale Energy and Reserve Markets*, IEEE Trans. Smart Grid, vol. 9, no. 4, pp. 3857-3870, Jul. 2018

[2] H. Gerard Vito and E. Rivero (Oct. 2017). Basic schemes for TSO-DSO coordination and ancillary services provision. Livermore, California. [Online]. Available: <https://api.semanticscholar.org/CorpusID:44683127>

[3] K. Oureilidis, K. N. Malamaki, K. Gallos, A. Tsitsmelis, C. Dikaiakos, et al., *Ancillary Services Market Design in Distribution Networks: Review and Identification of Barriers*, Energies, vol. 13, pp. 997, Feb. 2020

[4] KU Leuven Energy Institute. The Current Electricity Market Design in Europe. [Online]. Available: <http://set.kuleuven.be>

[5] J. F. Benders, *Partitioning procedures for solving mixed-variables programming problems*, J. Numer. Math., vol. 4, no. 1, pp. 238-252, 1962.

[6] J. W. Chinneck and K. Ramadan, *Linear programming with interval coefficients*, J. Oper. Res. Soc., vol. 51, no. 2, pp. 209-220, 2000.

[7] A. C. Rueda-Medina and A. Padilha-Feltrin, *Distributed generators as providers of reactive power support - A market approach*, IEEE Trans. Power Syst., vol. 28, no. 1, pp. 490-502, Feb. 2013.

[8] IEEE/PES. (2001, Feb.). Distribution Test Feeders. 37-bus Feeder. [Online]. Available: <http://ewh.ieee.org/soc/pes/dsacom/testfeeders/index.html>

[9] J. Wang, J. Xu, D. Ke, S. Liao, Y. Sun, J. Wang, et al., *A tri-level framework for distribution-level market clearing considering strategic participation of electrical vehicles and interactions with wholesale market*, Appl. Energy, vol. 329, pp. 120230, Jan. 2023

[10] T. Jiang, C. Wu, R. Zhang, et al., *Flexibility clearing in joint energy and flexibility markets considering TSO-DSO coordination*, IEEE Trans. Smart Grid, vol. 14, no. 2, pp. 1376-1387, Mar. 2023

[11] M. Mousavi, M. Wu, *A DSO Framework for Market Participation of DER Aggregators in Unbalanced Distribution Networks*, IEEE Trans. Power Syst., vol. 37, no. 3, pp. 2247-58, May 2021.

[12] A. R. Jordehi, V. S. Tabar, M. A. Jirdehi, *A two-stage stochastic model for security-constrained market clearing with wind power plants, storage systems and elastic demands*, J. Storage Mater., vol. 51, pp. 104550, Apr. 2022.

[13] IBM ILOG Division. (2022, May). IBM ILOG AMPL User’s Guide Including CPLEX Directives. International Business Machines Corporation IBM Co. Armonk. New York. [Online]. Available: <http://ampl.com/BOOKLETS/amplplex122userguide.pdf>

[14] J. C. do Prado, W. Qiao, *A stochastic distribution system market clearing and settlement model with distributed renewable energy utilization constraints*, IEEE Systems Journal, vol. 16, no. 2, pp. 2336-2346, Apr. 2021

[15] H. Chen, L. Fu, R. Zhang, et al., *Local energy market clearing of integrated ADN and district heating network coordinated with transmission system*, Int. J. Electr. Power Energy Syst., vol. 125, pp. 106522, Feb. 2021

[16] M. S. H. Nizami, M. J. Hossain, K. Mahmud, *A nested transactive energy market model to trade demand-side flexibility of residential consumers*, IEEE Trans. Smart Grid, vol. 12, no. 1, pp. 479-90, Jul. 2020

[17] J. M. Guerrero, M. Chandorkar, T. Lee, P. C. Loh, *Advanced control architectures for intelligent microgrids - Part I: Decentralized and hierarchical control*, IEEE Trans. Industrial Electron., vol. 60, no. 4, pp. 1254-1262, Apr. 2013.

[18] R. Cespedes, *New method for the analysis of distribution networks*, IEEE Trans. Power Del., vol. 5, no. 1, pp. 391-396, Aug. 1990.

[19] A. C. Rueda-Medina, J. F. Franco, M. J. Rider, A. Padilha-Feltrin, R. Romero, *A mixed-integer linear programming approach for optimal type, size and allocation of distributed generation in radial distribution systems*, Electric Power Systems Research, vol. 97, pp. 133-143, Apr. 2013.

[20] J. F. Manwell, J. G. McGowan, and A. L. Rogers, *Wind Energy Explained*, 2nd ed., New York, NY: Wiley, 2009, pp.23-84.

[21] M. Mahdavi, H. H. Alhelou and M. R. Hesamzadeh, *An Efficient Stochastic Reconfiguration Model for Distribution Systems With Uncertain Loads*, IEEE Access, vol. 10, pp. 10640-10652, Jan. 2022.

[22] R. Fourer, D. M. Gay and B. W. Kernighan, *Linear Programs: Variables, Objectives and Constraints*, in AMPL: A modeling language for mathematical programming, 2nd ed., vol.1, Pacific Grove, CA: Brooks/Cole-Thomson Learning, 2003, pp.129-137.